CO Time-History Measurements and Kinetic Modeling of Trimethyl Phosphate Pyrolysis

Keisuke Kanayama[1], Claire Grégoire[2], Kaoru Maruta[1], Eric L. Petersen[2], Olivier Mathieu[2], Hisashi Nakamura[1]
[1] Institute of Fluid Science, Tohoku University
Sendai, Miyagi, Japan
[2] J Mike Walker '66 Department of Mechanical Engineering, Texas A&M University
College Station, Texas, USA

1 Introduction

Organophosphorus compounds (OPCs) have been gaining attention as a fire-retardant additive to lithium-ion battery (LIB) electrolytes, thanks to their liquid physical properties, such as low vapor pressure as compared to carbonate ester solvents, and gas-phase phosphorus chemistry, a catalytic cycle that captures H/OH radicals [1,2]. To effectively suppress LIB fire incidents with OPC fire-retardant additives, understanding their combustion chemistry is important. Trimethyl phosphate (TMP) is one of the promising OPC fire-retardant candidates for a LIB electrolyte additive. The molecular structure of TMP resembles dimethyl carbonate (DMC), a commercially used electrolyte solvent component, as shown in Figure 1, only the center C-atom is substituted with a P-atom with an additional methoxy group. The role of TMP addition in hydrocarbon flames has been investigated (e.g., [1]), whereas its combustion chemistry, including the pyrolysis mechanism, seems to still require more development [3] for better model prediction as well as for systematic understanding of the difference in the efficiency among OPC fire-retardants, such as dimethyl methylphosphonate (DMMP).

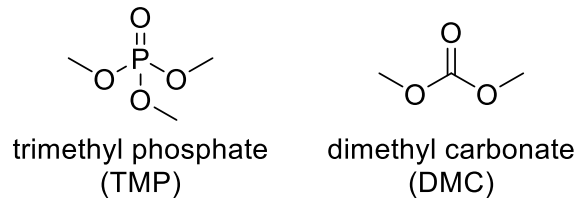

Figure 1: Molecular structures of trimethyl phosphate (TMP) and dimethyl carbonate (DMC).

The present study aims to validate TMP chemical kinetic models by obtaining the first CO time-history data for neat TMP pyrolysis. Shock-tube CO laser absorption measurements were conducted for TMP pyrolysis highly diluted with He/Ar mixtures at a temperature range of 1301–1695 K and near atmospheric pressure. A tentative chemical kinetic model of TMP pyrolysis is constructed upon a LIB electrolyte surrogate model [4] aiming at a future incorporation of a TMP sub-mechanism.

Correspondence to: keisuke.kanayama.a8@tohoku.ac.jp

2 Methods

2.1 Shock-Tube Configuration and CO Laser Absorption Diagnostic

The experimental study of TMP was carried out at Texas A&M University in a stainless-steel shock tube heated to a uniform temperature of 60°C using a custom-made jacket. Additional heating elements and fiberglass insulation set at 70°C were applied on the critical components, e.g., the mixing tank, the manifold, and the vial containing the phosphorus compound. The TMP was introduced in a vial and was degassed several times to ensure no air was introduced into the mixture. The TMP in the vapor phase was introduced in the mixing tank well below its maximum vapor pressure (0.83 Torr at 20°C, 30 Torr at 60°C). The highest partial pressure of TMP involved herein was 3.93 Torr to guarantee no fuel condensation occurring during the mixture preparation, defined as 0.0025 TMP/0.2 He/0.7975 Ar. The TMP came from Sigma Aldrich with a purity of 99%, and the gases, He and Ar, were provided by Praxair, all with 99.999% purity.

The shock tube consists of a driver section (7.62-cm inner diameter and 3.25-m long) and a driven section (16.2-cm inner diameter and 7.88-m long) separated by a single polycarbonate (0.25-mm thickness) diaphragm. Five PCB P113A22 piezoelectric pressure transducers, spaced on the sidewall along the end of the driven section, measured the passage of the shock wave, allowing the extrapolation of the shock wave velocity at the endwall location (v_s). The post-reflected-shock conditions, namely T_5 and P_5, are calculated using the 1-D normal shock equations using the initial temperature and pressure conditions (T_1 and P_1), v_s, and the initial mole fractions of the mixture. This method allows for a determination of T_5 and P_5 within ±0.8% and ±1.0%, respectively [5]. The high purity for these experiments is maintained with a vacuum system (a vane pump and a turbomolecular pump) to reach a pressure of 10^{-8} atm prior to each experiment. More details on the shock tube can be found in Mathieu et al. [6]. Finally, the experimental results were obtained for temperatures ranging from 1301 to 1695 K, and pressures ranging from 1.24 to 1.35 atm for φ = ∞ in 0.2 He/0.7975 Ar.

Quantitative CO concentration time histories behind reflected shock waves were recorded using a quantum cascade laser centered at 2059.91 cm^{-1} to monitor the P(20) line of the 1 ← 0 band for CO. The laser is centered on the wavelength using the maximum absorption strength with a removable cell containing a low-pressure mixture of CO in 90% Ar prior to each experiment. This laser technique has proven to work in relative isolation of any major products that could create interferences in the signals, such as H_2O and CO_2 [7]. The laser beam was split into two components: the time-resolved incident intensity I_0 and the time-resolved transmitted intensity I_t that passes through the reacting gases in the shock tube, both collected in InSb detectors. These intensities are processed with the Beer-Lambert relation to obtain the CO concentrations X_{CO}:

$$I_t/I_0 = \exp(-k_\nu P L X_{CO}),$$

where P is the partial pressure, L the path length, and k_ν the absorption coefficient, calibrated for temperatures between 1180 and 2190 K:

$$k_\nu = 23.78 \exp(-0.000646\, T).$$

2.2 Chemical Kinetic Modeling of TMP Pyrolysis

In this study, the pyrolysis section of the TMP model by Jayaweera et al. [8] was updated because there was a large discrepancy between experimental and computational results using the literature model, which is discussed in the next section. A LIB electrolyte surrogate model [4] in which C_0–C_2 chemistry from NUIGMech 1.1 [9,10] is implemented was used as a base model. Phosphorus chemistry including the TMP sub-mechanism was taken from the literature model by Jayaweera et al. [8] with some modifications in TMP and its related species' unimolecular decomposition reactions. Two TMP unimolecular decomposition reactions, a CH_3 loss channel and a CH_3O loss channel, were replaced or

removed by four unimolecular decomposition reactions proposed in our recent TMP thermal decomposition study [3]:

$$PO(OCH_3)_3 \rightarrow PO(OH)OCH_3(OCH_2) + CH_3 \quad \text{(R1170)}$$

$$PO(OCH_3)_3 \rightarrow P(OH)(OCH_3)_2 + CH_2O \quad \text{(R1171)}$$

$$PO(OCH_3)_3 \rightarrow CH_3OPO_2 + CH_3OCH_3 \quad \text{(R1172)}$$

$$PO(OCH_3)_3 \rightarrow PO(OCH_3)_2O + CH_3 \quad \text{(R1173)}$$

$PO(OCH_3)_3$ denotes TMP, and the reaction numbers correspond to those in the present TMP pyrolysis model. The rate parameters of R1170–R1173 were obtained by fitting the calculated rate constants [3] to the modified Arrhenius expression. An initial isomerization step for R1170 and R1171, $PO(OCH_3)_3 \leftrightharpoons P(OH)(OCH_2)(OCH_3)_2$, is not explicitly described in the present model. As the bond dissociation energy of P–OCH_3 is much larger than that of PO–CH_3, e.g., 111.9 kcal/mol and 87.5 kcal/mol calculated at the G4 level of theory [3], respectively, the TMP unimolecular reaction forming $PO(OCH_3)_2$ and CH_3O is not included in the present model. A subsequent reaction of $P(OH)(OCH_3)_2$, product of R1171, was determined based on analogy to $P(OH)CH_3(OCH_3)$:

$$P(OH)(OCH_3)_2 \leftrightharpoons CH_3OH + CH_3OPO \quad \text{(R1174)}$$

with the rate constant of R1174 being doubled from $P(OH)CH_3(OCH_3) \leftrightharpoons CH_3OH + CH_3PO$ because of two methoxy groups in the $P(OH)(OCH_3)_2$. Additionally, rate constants of phosphorus-containing intermediates' reactions, $PO(OCH_3)_2 \leftrightharpoons CH_3OPO_2 + CH_3$ (R1082) and $PO(OH)(OCH_3) \leftrightharpoons HOPO_2 + CH_3$ (R1112) were modified based on analogy to the PO–CH_3 bond fission of $POCH_3(OCH_3)$. The present TMP pyrolysis model involves 210 species and 1185 reactions including carbonate esters such as DMC, diethyl carbonate (DEC), ethyl methyl carbonate (EMC), and ethylene carbonate (EC).

3 Results and Discussion

Figure 2 shows the experimental CO time-history profiles for TMP pyrolysis at 1301–1695 K and near atmospheric pressure. Note that the spikes appearing before and at 0 μs correspond to a temporary laser beam steering caused by the density change from the passage of the incident and reflected shock waves, respectively. The measured CO mole fractions keep increasing in all temperature cases studied. At lower temperatures (1301 K and 1353 K), the CO profile gradually increases with its gradient growth within the measured time frame. This growth in the increasing rate is relaxed after around 1000 μs in the 1433 K case, followed by almost a linear increase. The change in the CO growth rate is more apparent at higher temperatures (1493 K, 1572 K, and 1695 K) where a rapid increase in the CO mole fraction appears between 0 and 500 μs, followed by a constant increase up to 2000 μs. The CO mole fraction at 1695 K after 2000 μs is around 3160 ppm, corresponding to 42% conversion of C-atom in TMP. Compared with the pyrolysis of DMC at a similar condition (0.25%DMC/20.00%He/79.95%Ar, 1664 K, 1.22 atm) [11], the CO time-history profile for DMC showed a rapid increase between 0–100 μs and a plateau afterwards (~ around 2600 μs), reaching the CO mole fraction of almost 2500 ppm. This case corresponds to the C-atom conversion of 33% when taking the center C-atom in the DMC molecule into account as well, while it marks 50% when only considering C-atoms constituting the methoxy groups. Thus, the conversion of C-atom from a methoxy group to CO is slightly lower for TMP than DMC, which may imply the possible formation of more hydrocarbons or OPC during TMP pyrolysis.

Figure 3 shows representative, experimental and computational CO time-history profiles at low, intermediate, and high temperatures. The literature model by Jayaweera et al. [8] underpredicts the CO mole fractions in the low- and intermediate-temperature cases over the measured time frame as shown in Figure 3a and 3b. It also underpredicts the onset of the initial, rapid increase in the CO profile for the high-temperature case, and turns into the overprediction of the CO mole fractions after 300 μs at 1695 K (Figure 3c). The discrepancy in the CO mole fraction at 1695 K between the literature model and the

experimental result enlarges as time proceeds. The present TMP model constructed in this study qualitatively reproduces CO profiles at all temperatures studied. Although the present model still slightly underpredicts the CO mole fractions at lower temperatures and overpredicts at higher temperatures, the overall trends are well captured, e.g., the constant CO increase at 1695 K after 500 μs.

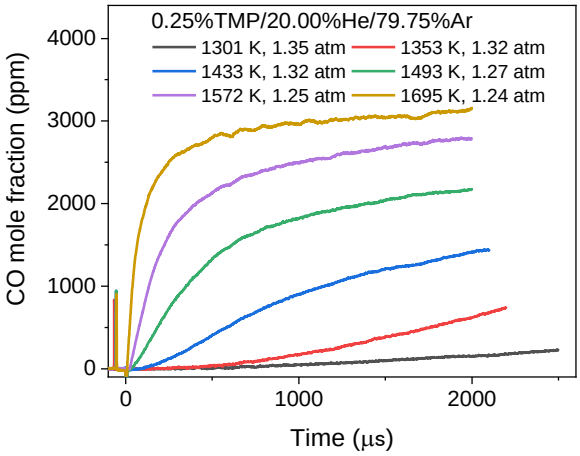

Figure 2: Experimental CO time-history profiles for TMP pyrolysis under 20.00%He/79.75%Ar dilution at 1301–1695 K and near atmospheric pressure.

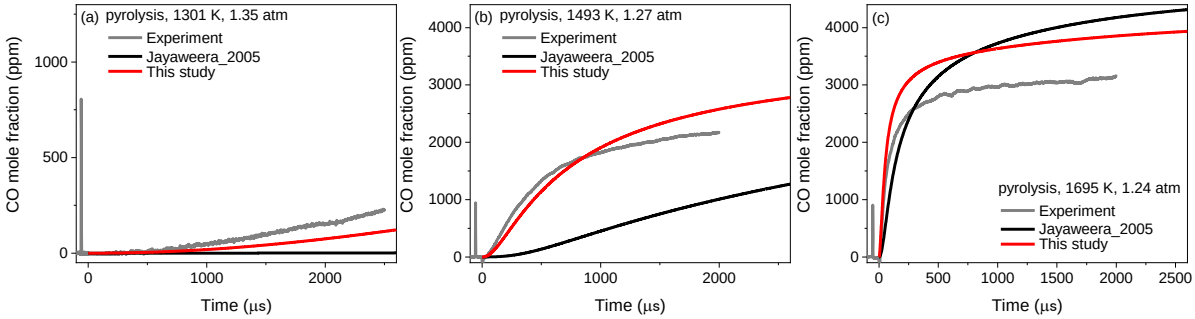

Figure 3: Representative CO time-history profiles for TMP pyrolysis at (a) 1301 K and 1.35 atm, (b) 1493 K and 1.27 atm, and (c) 1695 K and 1.24 atm. Experiments (grey) and computations using a model by Jayaweera et al. (black) and this study (red).

By conducting a rate of production analysis, CO was found to be produced mostly through HCO + M ⇋ H + CO + M (R187) in all the temperature cases studied. At intermediate- and high-temperature cases, there is a small contribution to the CO formation by $CH_2O + H \rightarrow H + CO + H_2$ (R186) in the time frame corresponding to the initial increase. For a further improvement of the model prediction, sensitivity analysis for CO mole fractions was performed, as shown in Figure 4. TMP unimolecular decomposition reaction of the PO–CH_3 bond cleavage directly producing CH_3 radicals, R1173, shows the highest sensitivity in all temperature cases (1301 K, 1493 K, and 1695 K). Another PO–CH_3 bond cleavage following an initial isomerization step of TMP, R1170, shows positive, high sensitivity as well. On the other hand, an H-atom abstraction reaction by H radical from TMP:

$$PO(OCH_3)_3 + H \leftrightharpoons PO(OCH_3)_2(OCH_2) + H_2 \qquad \text{(R1176)}$$

shows negative sensitivity in all temperature cases. Other highly sensitive reactions to CO mole fractions common to all temperature cases are those involving CH_2O or HCO, all possessing positive coefficients.

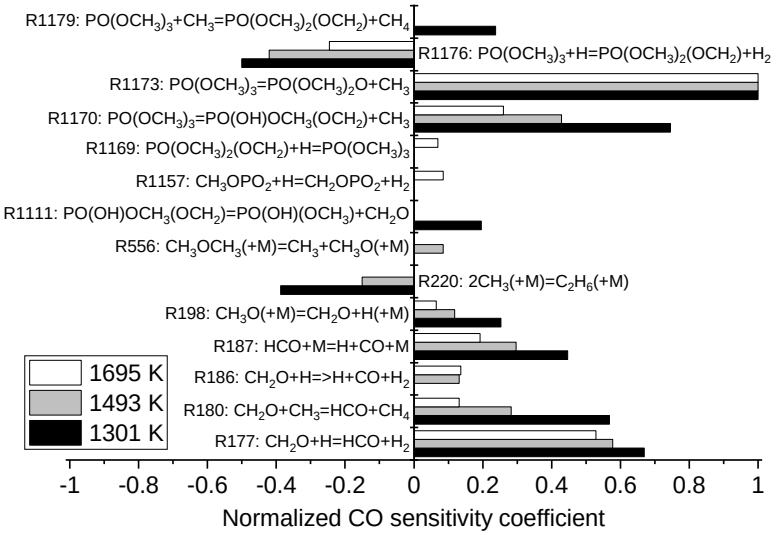

Figure 4: Normalized CO sensitivity coefficients for TMP pyrolysis at 1301 K, 1493 K, and 1695 K using the present TMP pyrolysis model. The top 10 reactions having the highest sensitivity values for each condition are presented.

At the lower temperature (1301 K), a decomposition reaction of $PO(OH)OCH_3(OCH_2)$ and a H-atom abstraction reaction of TMP by CH_3 show positive sensitivity:

$$PO(OH)OCH_3(OCH_2) \leftrightharpoons PO(OH)(OCH_3) + CH_2O \qquad (R1111)$$

$$PO(OCH_3)_3 + CH_3 \leftrightharpoons PO(OCH_3)_2(OCH_2) + CH_4 \qquad (R1179)$$

Due to the high branching ratio of R1170, which produces $PO(OH)OCH_3(OCH_2)$, in the TMP unimolecular decomposition reactions at relatively lower temperatures [3], R1170 as well as its subsequent reaction R1111 are more sensitive to CO mole fractions at lower temperatures as compared to intermediate- and high-temperature cases. For the intermediate temperature (1493 K), the TMP unimolecular decomposition pathways show a relatively high branching ratio in favor of the reaction producing dimethyl ether (DME), R1172, leading to the high sensitivity of a DME decomposition reaction:

$$CH_3OCH_3 (+ M) \leftrightharpoons CH_3 + CH_3O \qquad (R556)$$

As temperature increases, the branching ratio of the direct CH_3 loss channel from TMP, R1173, becomes dominant. A subsequent reaction of the phosphorus-moiety product of R1173, $PO(OCH_3)_2O$, proceeds via P–OCH_3 β-scission, producing CH_3OPO_2 and CH_3O. This may lead to a CH_3OPO_2 reaction:

$$CH_3OPO_2 + H \leftrightharpoons CH_2OPO_2 + H_2 \qquad (R1157)$$

having high sensitivity at the high temperature (1695 K). In addition, a reverse reaction of a H loss channel from TMP shows high sensitivity only at 1695 K:

$$PO(OCH_3)_3 \leftrightharpoons PO(OCH_3)_2(OCH_2) + H \qquad (-R1169)$$

The above reactions, especially those involving phosphorus-containing species, such as H-atom abstraction reactions from TMP (R1176 and R1179) and reactions related to phosphorus-containing intermediates (R1111 and R1157), would be possible candidates to be revised for their rate constants to improve the model prediction for the CO time-history profile. The present TMP pyrolysis model still needs to be elaborated and expanded to TMP oxidation before incorporating a TMP model with a LIB electrolyte surrogate model. More experimental data obtained with various methods and conditions are also important to further update the model as well as to understand the TMP pyrolysis mechanism.

4 Conclusions

CO time-history profiles during neat TMP pyrolysis were obtained using a shock tube with a CO laser absorption diagnostic at 1301–1695 K and near atmospheric pressure. Experimental CO time-history profiles at lower temperatures (e.g., 1301 K) gradually increase within the measured time frame, while those at higher temperatures (e.g., 1695 K) rapidly increase at the beginning, followed by a constant, slow growth within the measured time frame, but did not reach a plateau. A tentative TMP pyrolysis model constructed in the present study qualitatively reproduced the experimental CO profiles. According to the sensitivity analysis, phosphorus chemistry, such as H-atom abstraction reactions from TMP and reactions involving phosphorus-containing intermediates, might primarily be responsible for a quantitative discrepancy between the experimental and computational results as they showed different contributions depending on a temperature range. Other types of experimental data of TMP pyrolysis will also be helpful for further validation and improvement of the model accuracy.

References

[1] Korobeinichev OP, Shvartsberg VM, Shmakov AG, Bolshova TA, Jayaweera TM, Melius CF, Pitz WJ, Westbrook CK, Curran H. Flame inhibition by phosphorus-containing compounds in lean and rich propane flames. Proc. Combust. Inst. 30: 2353.

[2] Guo F, Ozaki Y, Nishimura K, Hashimoto N, Fujita O. Experimental study on flame stability limits of lithium ion battery electrolyte solvents with organophosphorus compounds addition using a candle-like wick combustion system. Combust. Flame 207: 63.

[3] Kanayama K, Nakamura H, Maruta K, Bodi A, Hemberger P. The Unimolecular Decomposition Mechanism of Trimethyl Phosphate. Chem. – A Eur. J. 30: e202401750.

[4] Kanayama K, Grégoire CM, Cooper SP, Almarzooq Y, Petersen EL, Mathieu O, Maruta K, Nakamura H. Experimental and chemical kinetic modeling study of ethylene carbonate oxidation: A lithium-ion battery electrolyte surrogate model. Combust. Flame 262: 113333.

[5] Petersen EL, Rickard MJA, Crofton MW, Abbey ED, Traum MJ, Kalitan DM. A facility for gas- and condensed-phase measurements behind shock waves. Meas. Sci. Technol. 16: 1716.

[6] Mathieu O, Mulvihill C, Petersen EL. Shock-tube water time-histories and ignition delay time measurements for H2S near atmospheric pressure. Proc. Combust. Inst. 36: 4019.

[7] Spearrin RM, Goldenstein CS, Jeffries JB, Hanson RK. Quantum cascade laser absorption sensor for carbon monoxide in high-pressure gases using wavelength modulation spectroscopy. Appl. Opt. 53: 1938.

[8] Jayaweera TM, Melius CF, Pitz WJ, Westbrook CK, Korobeinichev OP, Shvartsberg VM, Shmakov AG, Rybitskaya IV, Curran HJ. Flame inhibition by phosphorus-containing compounds over a range of equivalence ratios. Combust. Flame 140: 103.

[9] Wu Y, Panigrahy S, Sahu AB, Bariki C, Beeckmann J, Liang J, Mohamed AAE, Dong S, Tang C, Pitsch H, Huang Z, Curran HJ. Understanding the antagonistic effect of methanol as a component in surrogate fuel models: A case study of methanol/n-heptane mixtures. Combust. Flame 226: 229.

[10] Baigmohammadi M, Patel V, Nagaraja S, Ramalingam A, Martinez S, Panigrahy S, Mohamed AAE-S, Somers KP, Burke U, Heufer KA, Pekalski A, Curran HJ. Comprehensive Experimental and Simulation Study of the Ignition Delay Time Characteristics of Binary Blended Methane, Ethane, and Ethylene over a Wide Range of Temperature, Pressure, Equivalence Ratio, and Dilution. Energy & Fuels 34: 8808.

[11] Grégoire CM, Cooper SP, Khan-Ghauri M, Alturaifi SA, Petersen EL, Mathieu O. Pyrolysis study of dimethyl carbonate, diethyl carbonate, and ethyl methyl carbonate using shock-tube spectroscopic CO measurements and chemical kinetics investigation. Combust. Flame 249: 112594.